

The Preparation of Ideally Ordered Flat H-Si(111) Surfaces

Maximiliano L. Munford¹, Robert Cortès and Philippe Allongue*

Laboratoire de Physique des Liquides et Electrochimie,
CNRS - UPR 15 conventionnée avec l'Université P & M Curie
4 place Jussieu, Tour 22, 75005 Paris, France

(Received October 1, 2000; accepted December 5, 2000)

Key words: silicon, anisotropic etching, surface structure, AFM

The conditions required to prepare ideal flat H-S(111) surfaces by chemical etching in 40% NH₄F are examined using *ex-situ* atomic force microscopy (AFM) observations. We compare the topography of samples when the polished and eventually the rough (back) sides of an n-type Si(111) wafer are exposed to an etching solution. It is demonstrated that using an oxygen-free solution and exposing the two faces to the etching solution are two essential conditions for obtaining a surface that is free of etch pits. The result is independent of the angle of the miscut. The influence of the direction of the miscut on the morphology of step edges is investigated using the correlation between images and XRD characterizations at grazing incidence.

1. Introduction

The preparation of atomically flat H-terminated Si(111) surfaces by chemical etching in buffered ammonium fluoride solution has attracted much interest during the last decade. Currently, potential applications of such substrates in nanotechnology are widely recognized due to their exceptional flatness, chemical homogeneity and stability and their wide use in microelectronics. Their application will however require a perfect surface that is free of etch pits and, if possible, with an ordered array of steps on a long-range scale, i.e., several tens of micrometers.

The different parameters leading to the flattening of H-terminated Si(111) surfaces have been slowly identified over the years. The most important one is certainly the pH of

*Corresponding author: pa@ccr.jussieu.fr

¹Permanent address: Laboratório de Filmes Finos e Superfícies, Departamento de Física, UFSC, Florianópolis, Brazil.

the etching solution, which must be raised to eight by using a concentrated ammonium fluoride solution to increase the anisotropy ratio of the etching reaction. Chabal and co-workers were the first to establish that flat (111) terraces develop this way.⁽¹⁾ However, the Fourier Transform Infrared (FTIR) spectroscopy results of Chabal and co-workers were restricted to tilted (111) faces.⁽²⁾ Independent UHV-STM observations revealed that terraces are systematically pitted on well-oriented samples.⁽³⁻⁴⁾ A tilt angle of 2–4° was necessary to obtain a perfect step flow etching of the surface.⁽⁴⁾

Recently, Wade and Chidsey⁽⁵⁾ demonstrated that the pitting is completely suppressed by sparging the etching solution with N₂ (this removes the oxygen dissolved in the etching solution). Fukidome *et al.*^(6a) used sulfite salts as oxygen scavenger. This reduces the residual oxygen concentration to few ppb^(6a) and significantly improves the long-range order of the surface structure. The method is so efficient that Si may be etched at room temperature in pure water, without adding any F⁻ or OH⁻ ions.^(6b) Using electrochemical measurements, our group⁽⁷⁾ demonstrated that the suppression of pitting is also connected to galvanic effects occurring between the unpolished and the polished (111) faces of the same wafer when it is immersed in the etching solution.

The next section gives a summary of recent studies by our group. Subsequently we discuss the experimental conditions that are required to prepare an atomically flat H-Si(111) surface with an ordered staircase structure. We present new results demonstrating that the long-range surface structure of etched H-Si(111), i.e., the step morphology and ordering, is strongly dependent on the angle and the direction of the miscut. Results indicate that the last parameter is most essential.

2. Brief Summary of Former Studies

Experimentally, it remains a challenge, from a pure chemical point of view, to prepare an etch pit-free (111) surface with a well-oriented wafer. One may distinguish three different atomic sites on an H-terminated Si(111) surface (see Fig. 1): terrace, step and kink sites, which are labeled as TM, SM for terrace and step monohydrides and SD for step dihydrides. As presented in a former study combining *in-situ* STM observations and Monte-Carlo simulations⁽⁸⁾ the rate of dissolution of Si atoms depends on the number of Si-Si bonds and the access of the Si-H bonds to reactants from the solution. Another essential parameter is, for a given pH, the electrochemical potential applied to the sample. Regardless of these details one expects $k_{TM} \ll k_{SM} \ll k_{SD}$ where the k 's are the reaction rates on the above defined sites.

As shown in Ref. 8 for silicon etching in NaOH, a quantitative determination of the k -values may be performed by combining real time *in-situ* STM observations and digital simulation. For etching at the free potential (n-type sample): $k_{SD} \sim 5$, $k_{SM} \sim 0.04$ and $k_{TM} \sim 10^{-3}$. Values are expressed in atoms per second. It was also found that k_{TM} is exponentially dependent on the applied bias, while k_{SM} and k_{SD} are essentially independent of the potential. A similar study is still needed for silicon etching in NH₄F. It can only be roughly inferred that the above values, must be divided by a factor of ten to account for the slower etching rate in this solution.⁽⁹⁾ Using such values, the simulations yield a surface that is

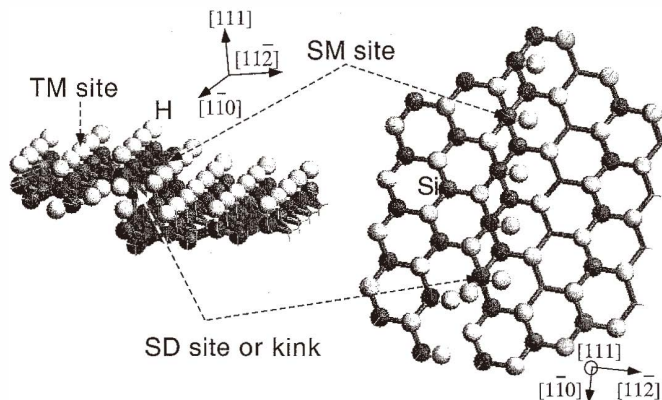


Fig. 1. 3D (left) and top view (right) ball and stick atomic structure of a step on an H-terminated Si(111) surface. Si and H atoms are respectively gray and light gray balls. The different atomic sites are identified as TM (terrace site), SM (step site) and SD (kinks).

pitted just like in the STM experiments: small flat (111) terraces develop but the long-range structure of the surface remains disordered.

As will be reported separately using Monte-Carlo simulation,^{*1} the complete suppression of pitting requires that the ratio k_{SD}/k_{TM} must be as large as 10^7 . A similar value has also been inferred by Hines and co-workers.⁽¹⁰⁾ Nevertheless, a difference in the reaction rates as large as seven orders of magnitude seems difficult to account for with simple considerations such as the atom coordination, the orientation of bonds and the steric hindrance (see Fig. 1). Thus we must examine "hidden" effects that were not considered previously. They are related to the technique of observation. *In-situ* STM imaging corresponds to a situation where dissolved oxygen is not removed from the cell and where only the polished (111) face is exposed to the solution. Reference 7 shows that this situation has a dramatic effect.

Figure 2 is a sketch of the model established for Si etching on the molecular scale.⁽¹¹⁾ The bottom route is considered to be electrochemical since it involves the injection of a free electron into the conduction band. This electron comes from an activated surface intermediate state.⁽¹²⁾ The top route is by contrast purely chemical. Both reactions lead to the formation of a Si-OH group which is then removed from the surface in a succession of chemical steps involving water molecules if the $\text{pH} > 4$.⁽¹¹⁾ Both reactions coexist at the open circuit potential (conditions of usual chemical etching) and their relative rates depend on the pH of the solution. Different studies have confirmed that the water molecules are the active species in Si etching while the OH^- or F^- ions are catalysts of the reaction. One study based its conclusion on the isotopic dependence of the etching rate, using H_2O or D_2O as solvent.⁽¹³⁾ The *in-situ* AFM observations of Si(111) etching in oxygen-free water at room temperature yield a more direct proof.⁽¹⁴⁾

In light of Fig. 2 one may qualitatively understand the site dependence of the reaction. The model was originally proposed for alkaline etching.⁽¹⁵⁾ In the initial stages, it also stands for NH_4F solutions except that the reaction is catalyzed by F^- ions and that the

*1 M. L. Munford, J. Kasparian and P. Allongue, in preparation for submission to Surface Science or Phys. Rev. B.

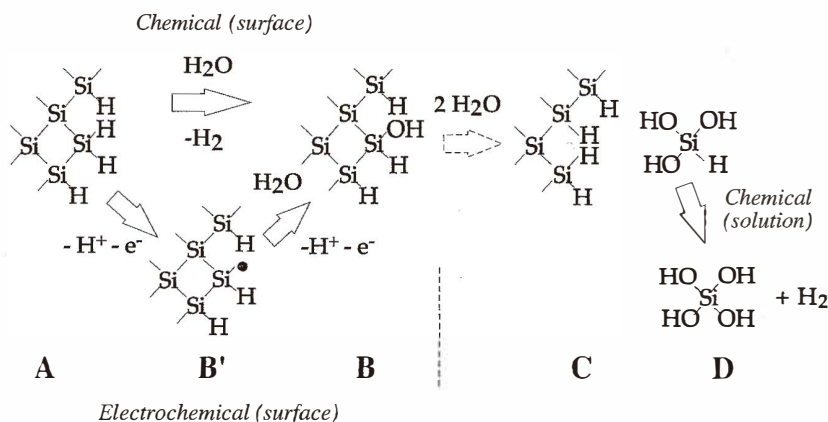


Fig. 2. Molecular model for the reaction of Si etching. After Refs. 10 and 16. Products are indicated with a (-) sign in front and reactants with no sign.

reaction intermediates are Si-F species after the initial hydrolysis step.⁽¹¹⁾ Two routes compete to initiate the dissolution process (step A \rightarrow B): one is purely chemical (top) and the second is electrochemical (bottom, via state B') while the remaining surface steps (B \rightarrow C) and solution reaction (C \rightarrow D) are common. In step A \rightarrow B, a water molecule is always involved and it must come in the close vicinity of the Si site. This is why, in the top route (i.e., the chemical reaction), the occurrence of the phenomenon is more probable at step edges where the Si-H bonds are nearly in plane whereas they are vertical on terrace. In contrast, the electrochemical path (bottom route) is expected to be much less site-dependent since state B' leaves free access to reaction with the water molecule.

The influence of the potential depends on the nature of the reaction. The electrochemical route is strongly bias-dependent and pitting is faster at anodic bias.⁽¹¹⁾ Under negative bias, the pitting is suppressed by the accumulation of a large density of electrons at the surface (case of an n-type electrode). This bias dependence was observed using *in-situ* STM imaging in NaOH.^(15a) Although a chemical reaction should be bias-independent, it is nevertheless observed that the accumulation of electrons at an n-Si surface impedes the reaction. The reason for this dependence is an electrostatic repulsion between the negatively charged surface and the doublet of electrons on the oxygen atom of the water molecule.^(15b)

Another important point that further slows down the kinetics of pitting on (111) terraces is the necessity of splitting the three Si-Si back bonds by insertion of water molecules.⁽⁸⁾ From a steric viewpoint, this should cause a large energy barrier due to elastic strains. The hard sphere diameter of a water molecule ($> 2.82 \text{ \AA}$)⁽¹¹⁾ is indeed greater than the Si-Si bond length (2.35 \AA). Splitting Si-Si bonds appears much easier at steps where some flexibility of bonds is expected.

3. Experimental

Silicon wafers were purchased from Siltronix (France). See the list in Table I. The H-terminated Si(111) surfaces were prepared using microelectronic grade chemicals. The samples were first cleaned in a boiling solution of H_2SO_4 and H_2O_2 (3:1 by volume) carefully rinsed in ultrapure water (UPW) and then immersed in 40% NH_4F for 20 min. They were then rinsed with UPW water sparged with nitrogen. Oxygen-free NH_4F was prepared by adding $(\text{NH}_4)_2\text{SO}_3$ so as to reach a concentration of 0.05 M.^(6a)

Contact-mode AFM imaging (Molecular Imaging, Tempe, USA) was performed under controlled N_2 atmosphere because the surfaces degraded quickly under the tip without this precaution. The typical spring constant of tips was 0.1–1 N/m. The images presented are typical ones. In other words, displacing the tip over a given sample or imaging another surface prepared with a Si crystal of the same batch gave similar surface topographies, particularly step morphology. All samples were characterized using grazing incidence XRD (5 circle custom setup) to precisely determine the angle and the direction of the miscut.

4. Results and Discussion

4.1 Characterization of the miscut

To correlate the surface topography to the way the crystal is cut, two angles must be considered. The first one is α , which defines the angle between [111] and the surface normal. It determines the average width of terraces. The second angle, θ is related to the tilt of the crystal in the orthogonal direction: θ is the angle between the projections on the plane of the surface of the vectors [111] and [11-2] (see Fig. 3(A)). In one simple case, where the [1-10] vector is in plane, $\theta = 180^\circ$. Only in this case, the terraces are expected to be ideally terminated by SM sites (i.e., the direction [11-2] is pointing out of the surface plane, Fig. 3(B)). For such a sample the miscut is said to be towards $\langle 11-2 \rangle$ since the projection of surface normal is oriented along [11-2]. At reverse, still with [1-10] in the surface plane, the terraces are expected to be SD-terminated when $\theta = 0^\circ$ (the direction \langle

Table 1.

List of n-type Si(111) samples studied in this paper. The angles α and θ are defined in Fig. 3A. The resistivity is the one given by the manufacturer. ψ is the angle, measured on AFM images, between [1-10] and the mean orientation of the steps.

Sample	Resistivity/ $\Omega\cdot\text{cm}$	α	θ	ψ
A	1500	0.13°	24°	52°
B	10	0.04°	25°	20°
C	0.23	0.24°	36°	25°
D	5–10	0.26°	162°	10°
E	10	0.17°	182°	$\sim 0^\circ$

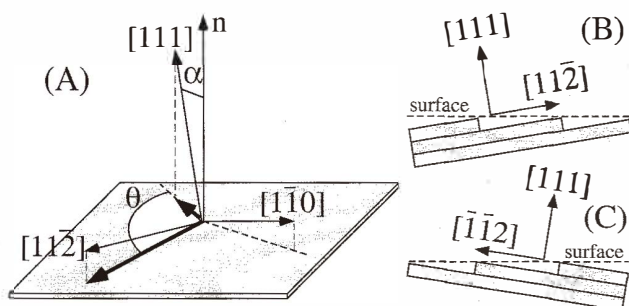


Fig. 3. Characterization of a Si(111) crystal. Case (A) : random miscut ($\alpha > 0$ and $0^\circ < \theta < 180^\circ$): Case (B) corresponds to Si-H-terminated steps ($\alpha > 0$ and $\theta = 180^\circ$): Case (C) corresponds to Si-H₂-terminated steps ($\alpha > 0$ and $\theta = 0^\circ$).

$1\text{-}12\rangle$ is pointing out of the surface plane, Fig. 3(C)). The miscut is said to be towards $[-1\text{-}12]$ in this case. When $0^\circ < \theta < 180^\circ$ there is a rotation of the crystal in the direction perpendicular to $[1\text{-}12]$: the vector $[1\text{-}10]$ is no longer in plane and steps contain kinks and SM sites in various proportions. This is the purpose of the following study to compare the morphology of the different surfaces.

4.2 Flattening of H-Si(111) surfaces: evidence of galvanic effects

As discussed in section 2, obtaining an ideally flat surface is apparently conflicting with STM experiments performed thus far. This prompted new investigations. In Fig. 4, we show the long-range topography of the etched H-Si(111) surface ($5 \times 5 \mu\text{m}^2$ AFM frames) in correlation with the experimental procedure used for etching. Sample E (Table I) was used. Its miscut of 0.2° is towards $[1\text{-}1\text{-}2]$ since $\theta \sim 180^\circ$ and SM steps are expected. All surfaces were etched for 20 min. Figure 4(a) shows that removing the oxygen by adding 50 mM of ammonium sulfite leads to a surface with a regular staircase structure where all steps are monatomic (3.14 \AA) and their mean separation distance (100 nm) is consistent with the miscut angle α (see inset). However, exposing only the (111) face to the solution, still in the strict absence of O₂, results in a surface with deep etch pits as shown in Fig. 4(b). On a smaller scale (inset), the terraces are atomically smooth with few etch pits and step edges are curved. There is no order even on this smaller scale. For comparison, we also report that if the 40% NH₄F solution contains dissolved oxygen, there is no chance of preparing an ordered surface even though the two faces are exposed to solution. Figure 4(c) is evidence of the existence of deep triangular etch pits when oxygen is present. However, this kind of structure was not found everywhere in the sample. By moving the tip across the sample surface (over several μm) we also observed regions with a greater density of deeper triangular etch pits.

The above observations are correlated to visual inspection of the sample during etching. It is well known that gas bubbles are evolving as the sample is etched.⁽²⁾ Figure 5 shows a

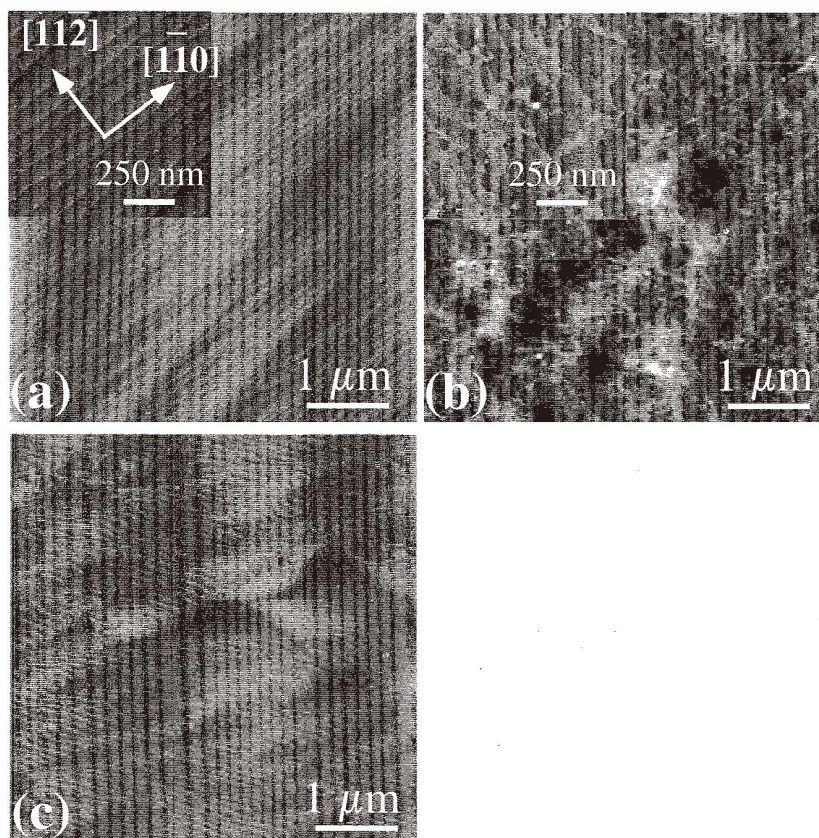


Fig. 4. ($5 \times 5 \mu\text{m}^2$) AFM images showing the surface of sample E (see Table I) etched under different experimental conditions: (A) the two faces of the wafer were exposed to an oxygen-free solution; (B) the (111) face alone was exposed to the solution; (C) same as (A) but in the presence of oxygen. Insets are $1 \times 1 \mu\text{m}^2$ close-up images.

series of pictures taken under the etching conditions of Fig. 4(a). The top row corresponds to the rough (rear) face and the bottom row to the polished (111) face. The sample was immersed with its oxide layer resulting from the cleaning procedure and positioned vertically in the hermetically sealed cell. After 2.5 min, gas bubbles become visible on the rear face only. They grow until coalescence and then detach from the surface when above a critical size. A new layer of gas bubbles forms immediately afterwards. Strong bubbling is also evident from the cleaved edges. In contrast, the (111) face remains almost free of gas bubbles during the 20 min of etching. The few bubbles observed on the polished face might even arise from the bottom edge of the sample.

The chemical nature of the gas evolved during etching is molecular hydrogen. This was experimentally verified in the case of KOH etching.⁽¹⁶⁾ Figure 2 shows that the dissolution

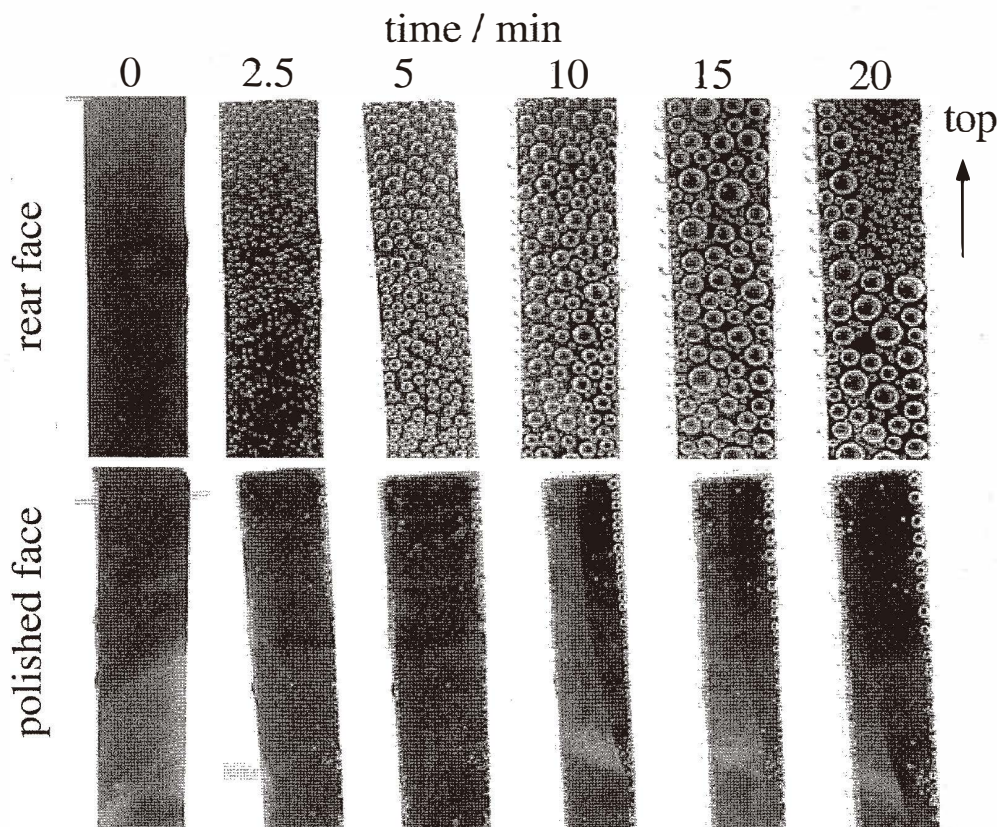


Fig. 5. Series of pictures taken during etching under the conditions defined in Fig. 4. The top and bottom rows correspond to the rear and (111) faces, respectively. The time is given in min. After cleaning, the silicon sample was immersed vertically in the solution and the beaker sealed.

of one silicon atom leads to the formation of one molecule of hydrogen.^{*1} Fukidome measured the etching rate by sampling the H_2 partial pressure in the atmosphere above the solution.^(6a) Qualitatively,^{*2} Fig. 5 is therefore a practical way for evaluating how fast and where the dissolution reaction is occurring on the silicon wafer: the etching is fastest at the rear face and the edges of the sample. The same experiment under the conditions of Fig. 4(b) (where only the polished face is exposed while the rough face is protected) leads, nevertheless, to significant gas evolution on the flat surface.^{*3} This indicates that there is a greater etching rate on the polished face under the conditions of Fig. 4(b) than when the two faces are exposed. With the chemical component (top route, in Fig. 2) being nearly independent of bias, we conclude that the electrochemical route (Fig. 2, bottom) is influenced by the experimental conditions (1 vs 2 faces exposed to the solution) through

^{*2}The formation of H_2 bubbles is a complex process which depends on several factors such as surface roughness, surface chemistry and also local saturation of the solution.

^{*3}For this experiment one needs to carefully protect the rear face and the edges of the samples, so as to expose only the (111) polished face.

galvanic effects. We postulate that the polished face is under cathodic protection when the two faces are in contact with the solution.^{*4} Electrochemical measurements confirm this assessment.^{(7),*1} In the presence of oxygen (case of Fig. 4(c)), the rate of bubble generation is only slightly faster than that observed in Fig. 5, with the rate on the rear face being still much greater than that on the (111) face.

4.3 Long-range step edge structure and surface order

A few years ago, there was a debate about the structure of steps, which were either jagged or straight depending on the miscut angle (angle α) and miscut direction.⁽³⁻⁴⁾ Figure 6 compares the surface morphology of different low-doped n-type crystals with different miscuts (see Table I). Compared to Fig. 4(a), where the steps are straight, it becomes clear

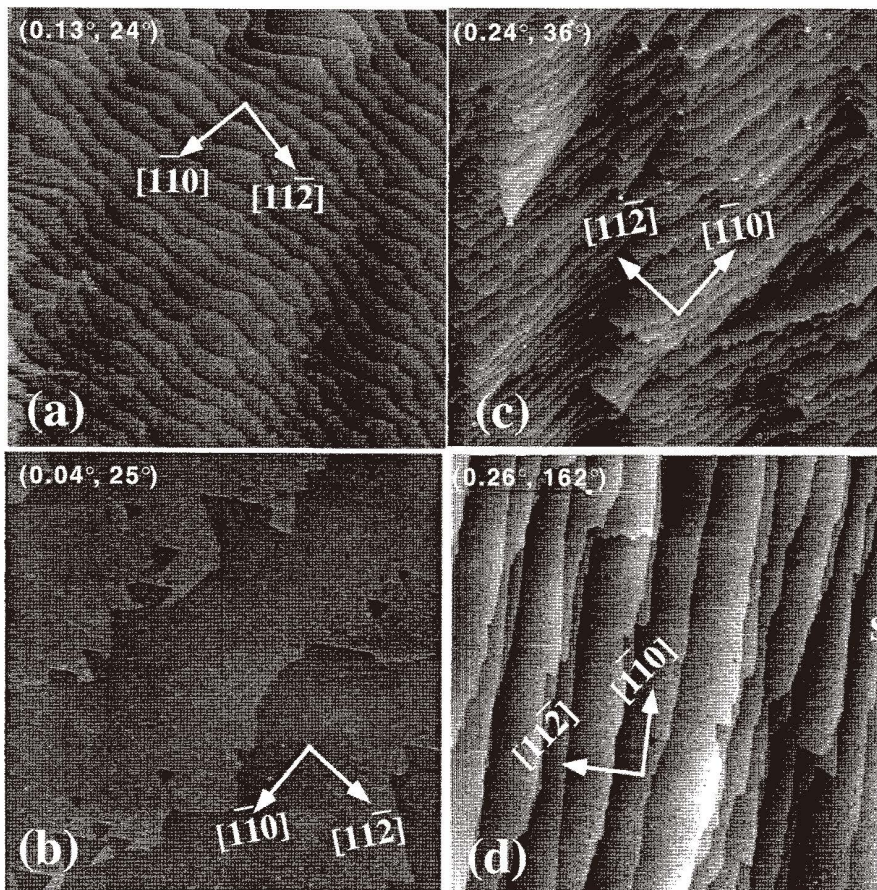


Fig. 6. ($2 \times 2 \mu\text{m}^2$) AFM images showing the structure of steps on different n-type low-doped substrates. Etching time : 20 min in all cases. Images (a-d) correspond respectively to samples (A-D) of Table I. The angles (α , θ) are indicated.

^{*4}The situation is equivalent to the one where the (111) face would be exposed to solution but polarized at a cathodic potential, just like in the STM experiments reported in Ref. 16.

that the direction of the miscuts, characterized by the angle θ (Fig. 3), is critically influencing the long-range structure of the steps. Perfectly straight steps are obtainable when the miscut direction is close to $[11-2]$ (Fig. 4(a), sample E). In this case, the steps are running parallel to the $[1-10]$ direction within $\sim 0^\circ$. They present few kinks with the resolution of the AFM images.

In all other cases, the disorder increases on the surface. Sample A (Fig. 6(a)) has a miscut, which is 24° off the right orientation. The steps are regularly spaced and only meander along a main direction which is 52° off $[1-10]$. Sample B (Fig. 6(b)) is cut in the same direction as sample A, but with a very small tilt angle $\alpha = 0.04^\circ$. The steps are, on average, 20° off $[1-10]$ and are partially jagged. The spacing between steps is still rather regular. Sample C (Fig. 6(c)) corresponds to the worst situation. The orientation of the miscut is 36° off $[11-2]$, i.e., it is in the middle of $[11-2]$ and $[-1-12]$, meaning that the steps are initially composed of alternating SD and SM sites. This results in the strongest disorder ever seen, with the steps containing many kinks and hillocks. Step bunching is also observed. The mean orientation of steps is 25° off $[1-10]$. Last, sample D (Fig. 6(d)) corresponds to a sample with a miscut towards $[11-2]$ but with 18° in-plane rotation. The order of the surface is improved. No hillock has formed. Some steps exhibit huge kinks while others are relatively straight (not kink-free however) and step agglomeration is also occurring in some places. The mean direction of steps is 10° off $[1-10]$.

From the above results, it is evident that the structure of terraces is independent of the direction of the miscut. In all images, the terraces are atomically smooth regardless of the α -value and the terrace width W is close to expectations, unless the θ -value is too close to a situation where hillocks are generated: namely $W (\text{\AA}) \sim 3.14 / \tan(\alpha)$. Terraces may extend over more than $1 \mu\text{m}$ without etch pits for $\alpha \sim 0.04^\circ$ (Fig. 6(b), sample C). This result, which contradicts previous observations [3-4] emphasizes the importance of removing the oxygen from the etching solution and also proves the efficiency of the cathodic protection of the (111) face induced by the rear face in contact with the solution (compare Fig. 4(b) and Fig. 6). This is the direction of the cut of the crystal which is the most critical factor influencing the long-range morphology of step edges and it becomes clear that manufacturers need to control this parameter on well-oriented wafers. At this stage of our study, there is no clear relationship between the mean orientation of steps and the angle θ . Digital simulations are necessary.

5. Conclusions

This work demonstrated that the conditions used during Si etching are extremely important regarding the long-range order of precisely oriented H-Si(111) surfaces. On an atomic scale, smooth terraces can be obtained with any n-type material, regardless of its doping level or miscut, provided that one carefully removes the oxygen and one exposes the two faces of the wafer to the etching solution. The long-range order of the surface, i.e., the ability to prepare a quasi-perfect staircase structure, is only dependent on the crystal cut. More specifically, the direction of miscut determines the step structure. These may be straight over several tens of micrometers if the direction of the miscut is precisely controlled and close to $\langle 11-2 \rangle$.

Acknowledgments

M. L. M gratefully thanks the CAPES (Brazil) for a scholarship obtained during his Ph. D. and the support of Professor A. A. Pasa (Department of Physics, Federal University of Santa Catarina in Florianopolis, Brazil). This work was partially financed by the Programme Matériaux of CNRS and the Direction des Affaires Internationales de l'Université P. & M; Curie (Paris).

References

- 1 G. S. Higashi, Y. J. Chabal, G. W. Trucks and K. Raghavachari: *Appl. Phys. Lett.* **56** (1990) 656.
- 2 P. Jakob and Y. J. Chabal: *J. Chem. Phys.* **95** (1991) 2897.
- 3 H. E. Hessel, A. Feltz, U. Memmert and R. J. Behm: *Chem. Phys. Lett.* **186** (1991) 275.
- 4 G. Pietsch, U. Köhler and M. Henzler: *J. Appl. Phys.* **73** (1993) 4797.
- 5 C. P. Wade and C. E. D. Chidsey: *Appl. Phys. Lett.* **71** (1997) 1679.
- 6 a) H. Fukidome: Ph. D. thesis, Osaka University (2000); b) H. Fukidome, M. Matsumura, T. Komeda, K. Mamba and Y. Nishika: *Electrochem. and Solid State Lett.* **2** (1999) 393.
- 7 P. Allongue, C. Henry de Villeneuve, S. Morin, R. Boukherroub and D. D. M. Wayner: *Electrochim. Acta* **45** (2000) 4591.
- 8 J. Kasparian, M. Elwenspoek and P. Allongue: *Surf. Sci.* **388** (1997) 50.
- 9 J. Kasparian and P. Allongue: *Electrochemical Society Meeting Proc. PV-97-20* (1997) p. 220.
- 10 J. Flidr, Y.-C. Huang, T. Newton and M. Hines: *J. Chem. Phys.* **108** (1998) 5542.
- 11 P. Allongue, V. Kieling and H. Gerischer: *Electrochim. Acta* **40** (1995) 1353.
- 12 H. Gerischer, P. Allongue and V. Costa-Kieling: *Ber. Bunsenges. Phys. Chem.* **97** (1993) 753.
- 13 T. Baum and D. J. Schiffrin: *J. Electroanal. Chem.* **436** (1997) 239.
- 14 H. Fukidome, M. Matsumura, T. Komeda, K. Namba and Y. Nishioka: *Electrochem. and Solid-State Lett.* **2** (1999) 393.
- 15 a) P. Allongue, V. Kieling and H. Gerischer: *J. Electrochem. Soc.* **140** (1993) 1008; b) P. Allongue, V. Kieling and H. Gerischer: *J. Electrochem. Soc.* **140** (1993) 1018.
- 16 E. D. Palik, O. J. Glmebocki and I. Heard Jr.: *J. Electrochem. Soc.* **134** (1987) 404.